Applied Catalysis B: Environmental 140–141 (2013) 708–715

Contents lists available at SciVerse ScienceDirect

Applied Catalysis B: Environmental

journal homepage: www.elsevier.com/locate/apcatb

Effect of V_2O_5 loading of V_2O_5/TiO_2 catalysts prepared via CVC and impregnation methods on NO_x removal

Woojoon Cha[a,b], Sungmin Chin[a], Eunseuk Park[a], Seong-Taek Yun[b], Jongsoo Jurng[a,b,*]

[a] Center for Environment, Health and Welfare Research, Korea Institute of Science and Technology (KIST), 39-1 Hawolgok, Seongbuk, Seoul 136-791, Republic of Korea

[b] Green School, Korea University-KIST, 145 Anam-ro, Seongbuk-gu, Seoul 136-701, Republic of Korea

ARTICLE INFO

Article history:
Received 25 January 2013
Received in revised form 22 March 2013
Accepted 3 May 2013
Available online 9 May 2013

Keywords:
V_2O_5/TiO_2
Chemical vapor condensation (CVC)
SCR
NO_x

ABSTRACT

In this study, V_2O_5/CVC-TiO_2 materials with different concentrations of V_2O_5 were prepared via chemical vapor condensation (CVC) and impregnation. The catalytic activities of these materials were tested and the physicochemical characteristics were analyzed using XRD, BET, FT-IR spectroscopy, XPS, HR-TEM, EDX mapping, H_2-TPR, and NH_3-TPD. The NO_x removal efficiency of the V_2O_5/CVC-TiO_2 catalysts was higher than that of the V_2O_5/P25-TiO_2 catalysts and increased with increasing V_2O_5 concentration. At 200 °C, the highest NO_x conversion was observed using 7 and 10 wt.% V_2O_5/CVC-TiO_2 catalysts. The NO_x conversion curve reached a plateau corresponding to the maximum conversion when the V_2O_5 content was greater than 7 wt.%. The V_2O_5/CVC-TiO_2 catalyst comprised mainly anatase-phase TiO_2 and well-dispersed V_2O_5. A greater concentration of V (well-balanced V^{4+}/V^{5+}) species existed on the V_2O_5/CVC-TiO_2 catalyst surface. H_2-TPR and NH_3-TPD testing confirmed that the V_2O_5/CVC-TiO_2 catalyst is highly reducible and has many acidic sites.

1. Introduction

Nitrogen oxides (NO_x) remain a major source of air pollution and contribute to photochemical smog, acid rain, ozone depletion, and greenhouse effects. The direct health hazards related to NO_x include bronchitis, pneumonia, viral infections, and hay fever [1]. Currently, selective catalytic reduction (SCR) of NO_x with NH_3 is one of the most efficient methods for reducing nitrogen oxide emissions from stationary sources such as incinerators [2].

Vanadia catalysts supported on titania have been widely employed for SCR of NO_x with NH_3 owing to its high catalytic activity and sulfur tolerance under actual flue-gas conditions [3,4]. NH_3-SCR catalysis in incinerators requires the removal of NO_x at low temperatures. Accordingly, a plethora of SCR catalysts have been studied in the literature, and V_2O_5/TiO_2 and V_2O_5–WO_3/TiO_2 catalysts have been widely applied. However, most of the catalysts must operate above 350 °C [5]. Among SCR catalysts, V_2O_5 supported on TiO_2 is generally recognized as the most active and selective catalyst within an appropriate temperature window [6,7]. Therefore, the development of new SCR catalysts that are active at temperatures far below 350 °C but high enough for chimney ventilation is required.

TiO_2 support materials for SCR DeNO_x catalysts can be manufactured via a variety of methods including hydrothermal, combustion flame, chemical vapor deposition, chemical vapor condensation, etc. Of these, chemical vapor condensation (CVC) is known to result in good catalytic properties. Specifically, Chin et al. [8,9] reported that TiO_2 prepared using the CVC method had a larger surface area with smaller particle sizes and more anatase-TiO_2 than commercial TiO_2 (Degussa, P25). These properties are beneficial for photocatalysts and support materials for heterogeneous catalysts. In addition, V_2O_5/TiO_2 catalysts synthesized using the CVC method comprise high-purity nanostructured powders that do not undergo agglomeration, with a grain size of less than 30 nm and a large surface area, and show high catalytic activity [9–12]; these catalysts showed better performance than the commercial catalyst, particularly at lower temperatures.

The impregnation method of preparing V_2O_5/TiO_2 catalysts enables control of the V_2O_5 loading and results in the highest NH_3-SCR activity at low temperatures. This suggests that the interaction of V_2O_5 with TiO_2 modifies the structural and chemical properties of V_2O_5 and imparts desirable catalytic properties [6,13]. Spreading vanadium over a TiO_2 support modifies the chemical and physical properties of vanadium and enhances its catalytic properties [14–16]. The structural characteristics and SCR activity of V_2O_5/TiO_2 depend mainly on the preparation method and conditions, such as TiO_2 structure and vanadium loading [17]. Further,

* Corresponding author at: Center for Environment, Health and Welfare Research, Korea Institute of Science and Technology (KIST), 39-1 Hawolgok, Seongbuk, Seoul 136-791, Republic of Korea. Tel.: +82 2 958 5688; fax: +82 2 958 6711.
E-mail address: jongsoo@kist.re.kr (J. Jurng).

0926-3373/$ – see front matter © 2013 Elsevier B.V. All rights reserved.
http://dx.doi.org/10.1016/j.apcatb.2013.05.002

the reducing effect of a reducing gas (NO_x) has been investigated using V_2O_5/TiO_2 catalysts produced with different loadings of vanadia: The amount of metal oxide loaded affects the reducing capacity [5,18]. Accordingly, V_2O_5/CVC-TiO_2 catalysts loaded with different amounts of V_2O_5 are anticipated to have different SCR activities toward NO_x removal at low temperature.

The aim of this study is to determine the optimal V_2O_5 loading concentration for maximum SCR activity at low temperature and investigates the effect of increased V_2O_5 content. Catalytic activity tests are performed using NH_3-SCR for NO_x removal. The chemico-physical properties of V_2O_5/TiO_2 catalysts with varying amounts of V_2O_5, which were prepared via CVC and impregnation methods, were analyzed using XRD, BET, FT-IR spectroscopy, XPS, HR-TEM, EDX mapping, H_2-TPR, and NH_3-TPD; the results are compared with those for commercial TiO_2 (i.e., P25).

2. Materials and methods

2.1. Catalyst preparation

The CVC method described in our previous study [19] was used to produce the TiO_2 nanoparticles. The titanium tetraisopropoxide (TTIP) precursor was synthesized at 900 °C; this temperature yielded the highest catalytic activity of the resultant TiO_2 nanoparticles. The catalysts synthesized by the CVC method are labeled "CVC-TiO_2," while the commercial catalyst (Degussa, P25) is labeled "P25-TiO_2." TiO_2-supported vanadium oxides were prepared using the impregnation method. Samples loaded with 1, 2, 5, 7, and 10 wt.% vanadium oxide were impregnated with stoichiometric amounts of ammonium-meta-vanadate (99.0%, NH_4VO_3, Samchun Chem.) dissolved in oxalic acid (97.0% $(COOH)_2$, Kanto Chem.). The catalyst samples were dried overnight at 110 °C then calcined at 500 °C for 2 h in static air. Next, each catalyst sample was crushed and ground into a powder with particle sizes of 250–850 μm.

2.2. Catalytic activity testing

The activity of the catalyst toward NH_3-SCR for NO_x removal was tested using a metallic fixed-bed reactor (5 mm i.d.). The catalyst samples were placed at the center of the reactor, and the temperature of the electric furnace was controlled using a temperature program controller. To simulate flue gas, the feed gas, which comprised 200 ppm NO, 200 ppm NH_3, and 5 vol.% O_2 with N_2 balance, was adjusted using a mass-flow controller and injected into the reactor at a total rate of 490 $cm^3\,min^{-1}$ with a gas hourly space velocity of 100,000 h^{-1}. The NO_x conversion was measured using a gas analyzer (MK9000, Ecom RBR) that could individually analyze NO, NO_2, and NO_x (NO + NO_2). The NO_x conversion is expressed via the following equation.

Equation for NO_x conversion (%).

$$NO_x \quad \text{conversion} = \frac{[NO]_{inlet} - [NO + NO_2]_{outlet}}{[NO]_{inlet}} \times 100\%$$

The N_2 selectivity and N_2O concentration measured was measured using an FTIR spectrometer (iS10, Thermo Fisher). The N_2 selectivity was calculated using an equation published by Shi et al. [29].

2.3. Characterization of catalysts

X-ray diffraction (XRD) patterns of the catalysts were obtained using a focal size of 5 mm^2 and a Cu rotating anode; the samples were scanned from 20° to 80° (2θ) at a rate of 2 min^{-1}. The powder specific surface areas (SSAs; m^2/g) were determined by nitrogen adsorption (>99.999%) at 77 K using a Micromeritics Tristar 3000 apparatus via the Brunauer–Emmett–Teller (BET) method. Fourier transform infrared (FT-IR) spectroscopy was performed using a spectrophotometer (Omars 89, Dilor) equipped with an intensified photodiode array detector and with a spectrometer (IFS110, Bruker). X-ray photoelectron spectroscopy (XPS) was used to observe the oxidation states of the metals on the surface; an AXIS-NOVA (Kratos Inc.) spectrometer with high-resolution scans using monochromatic Al Kα radiation (1486.6 eV), a step size of 0.05 eV, and an abide time of 100 $m\,s^{-1}$ was used. High-resolution transmission electron microscopy (HR-TEM) and energy-dispersive X-ray (EDX) mapping were performed using an F-20 microscope (Philips) operated at 200 kV with an image resolution of 0.25 nm. Temperature-programmed reduction (TPR) runs were carried out with linear heating at 10 °C/min up to 800 °C in 5% H_2 in Ar flowing at 30 mL/min. Hydrogen consumption during TPR was measured using a thermal conductivity detector (TCD; model: BELCAT-M, BEL Japan, Inc.), which was also used for the NH_3 temperature-programmed desorption (TPD) runs.

3. Results and discussion

3.1. NH_3-SCR activity test

There was negligible conversion of NO_x over pure CVC-TiO_2 and P25-TiO_2 supports at any temperature (results not shown here); however, dispersing V_2O_5 onto TiO_2 generally improved the activity toward the SCR of NO_x. Fig. 1(a) shows that the SCR results correlate with the catalytic activity of the 5 and 7 wt.% V_2O_5/TiO_2 catalysts. The NO_x conversion efficiencies of the 7 wt.% V_2O_5/CVC-TiO_2 and V_2O_5/P25-TiO_2 catalysts were 96% and 82%, respectively, while those of the 5 wt.% V_2O_5/CVC-TiO_2 and V_2O_5/P25-TiO_2 catalysts were 70% and 68%, respectively. The temperature ranges for the highest NO_x removal efficiencies were ~200–350 °C (7 wt.% V_2O_5/CVC-TiO_2), ~300–350 °C (7 wt.% V_2O_5/P25-TiO_2), ~250–350 °C (5 wt.% V_2O_5/CVC-TiO_2), and ~300–350 °C (5 wt.% V_2O_5/P25-TiO_2). It is noteworthy that the NO_x conversion efficiencies of the V_2O_5/CVC-TiO_2 catalysts were greater than 90% at lower operating temperatures (i.e., ~200–250 °C), while those of the V_2O_5/P25-TiO_2 catalysts were less than 86% at the same operating temperatures. To achieve a NO_x conversion efficiency of 96%, the required operating temperature of the 7 wt.% V_2O_5/CVC-TiO_2 catalyst was about 50 °C lower than that of the 5 wt.% V_2O_5/CVC-TiO_2 catalyst. At 200 °C, the V_2O_5/CVC-TiO_2 catalysts with varying concentrations of V_2O_5 showed sufficient NO_x conversion, while the NO_x conversion efficiencies of the V_2O_5/P25-TiO_2 catalysts with the same V_2O_5 concentrations were insufficient. We propose that the V_2O_5/CVC-TiO_2 catalysts had more anatase-phase TiO_2, a higher specific surface area, and better dispersion than the V_2O_5/P25-TiO_2 catalysts. Sufficiently high NO_x conversion efficiency was achieved using the V_2O_5/TiO_2 catalyst with greater than 7 wt.% V_2O_5 loading.

The results of SCR at 200 °C with V_2O_5 loadings from 1 to 10 wt.% are shown in Fig. 1(b): All V_2O_5/CVC-TiO_2 catalysts were more active that V_2O_5/P25-TiO_2 for NO_x conversion. The NO_x conversion efficiencies of the V_2O_5/CVC-TiO_2 catalysts were 10, 43, 71, 96, and 96% with 1, 2, 5, 7, and 10 wt.% vanadia loading on the CVC-TiO_2 surface, respectively. The NO_x conversion efficiency linearly increases with increasing V_2O_5 loading from 1 to 7 wt.%. These results suggest that more vanadia active sites are present when more vanadia is loaded onto the CVC-TiO_2 surface. However, the NO_x conversion remained constant upon further increasing the V_2O_5 loading from 7 to 10 wt.%. We postulate that the number of active sites on the CVC-TiO_2 surface was saturated at 10 wt.% and the excess vanadia existed in an improper state such as a bulk (crystallized) phase. Among these catalysts, the 7 wt.% V_2O_5/CVC-TiO_2 catalyst showed the highest NO_x conversion efficiency (96%) at low temperatures.

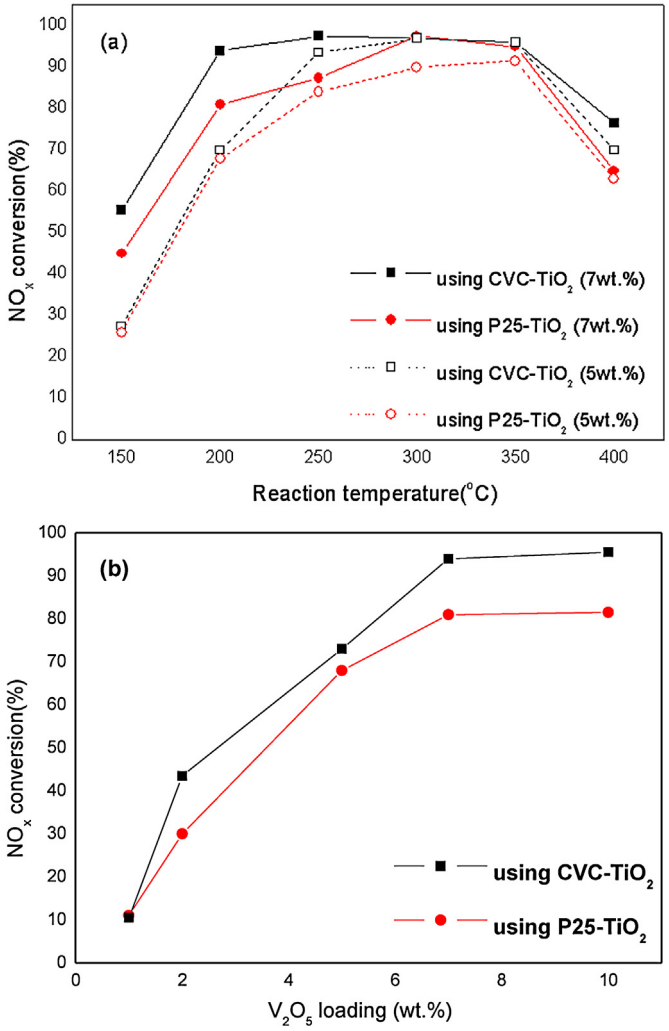

Fig. 1. Results of NH_3-SCR activity testing of V_2O_5/TiO_2 catalysts for $DeNO_x$. (a) NO_x conversion with 5 and 7 wt.% V_2O_5/TiO_2 catalysts using CVC-TiO_2 and P25-TiO_2 supports; (b) NO_x conversion with V_2O_5/TiO_2 with varied V_2O_5 loading concentrations (i.e., 1, 2, 5, 7, and 10 wt.%) at 200 °C.

The N_2 selectivity and N_2O concentration of all samples was nearly 100% irrespective of the catalytic activity below 300 °C (Fig. 2). However, the N_2O concentrations and N_2 selectivities of 7 wt.% V_2O_5/CVC-TiO_2 and V_2O_5/P25-TiO_2 were about 4 ppm and

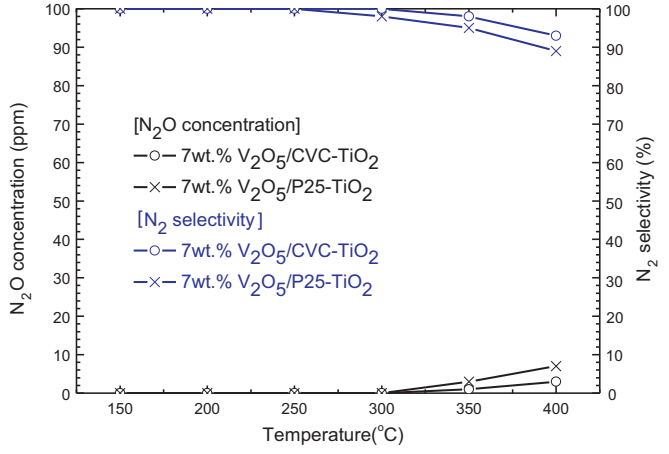

Fig. 2. N_2O concentrations and N_2 selectivity during the NH_3-SCR process.

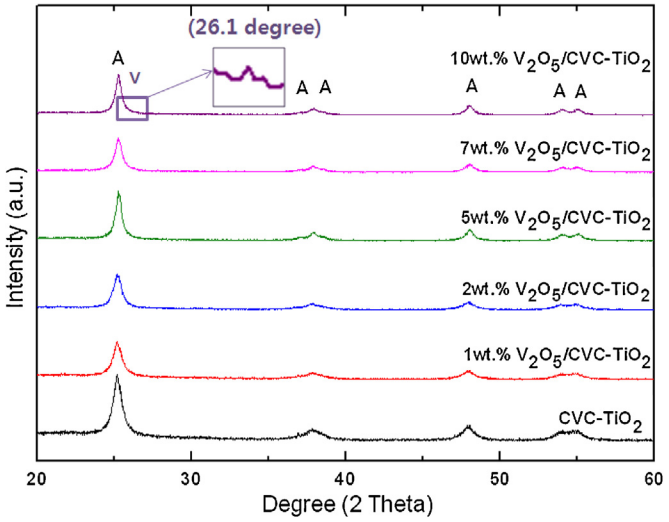

Fig. 3. XRD patterns of CVC-TiO_2 and V_2O_5/CVC-TiO_2 samples with different concentrations of V_2O_5 (i.e., 1, 2, 5, 7, and 10 wt.%). The symbols 'A' and 'V' indicate anatase and V_2O_5, respectively.

93% and 8 ppm and 88%, respectively, at 400 °C. Shi et al. [29] reported that the N_2 selectivity and amount of N_2O generated decreased during the NH_3-SCR process above ~400–450 °C.

3.2. Catalyst characterization

3.2.1. Textural properties

XRD was used to determine the bulk crystalline phases in the nanoparticle samples. The diffraction patterns ($20° < 2\theta < 60°$) of the V_2O_5/CVC-TiO_2 materials containing various concentrations of V_2O_5 showed only amorphous anatase peaks: No rutile peak was detected (Fig. 3). V_2O_5 peaks are not evident in the XRD results even with increasing V_2O_5 content from 1 to 7 wt.%. This result suggests that that V_2O_5 is amorphous, well-dispersed onto the CVC-TiO_2 surface, and does not crystallize; this results in improved catalytic NO_x removal, as it provides an increased number of active sites. As reported previously, vanadium oxide would be amorphous [25], and the low crystallinity and good dispersion of the active phase is favorable for catalytic activity [26]. However, at 10 wt.% V_2O_5, a V_2O_5 peak appeared at ~26.1°, which suggests that V_2O_5 transforms from monomeric or polymeric forms to a bulk form via crystallization. Bulk (i.e., crystallized) V_2O_5 has fewer active sites than monomeric or polymeric V_2O_5 resulting in reduced SCR activity. The negligible effect of increasing the V_2O_5 loading above 7 wt.% on the SCR activity (Fig. 1(b)) is attributed to this phenomenon. At the concentration of V_2O_5 that V_2O_5 peaks were detected via XRD, the catalytic activity was either stabilized or inferior at a low reaction temperature [27].

When V_2O_5 is loaded onto CVC-TiO_2 to prepare catalysts, anatase-TiO_2 does not transform to rutile-TiO_2. As reported previously [20], anatase-TiO_2 transforms to rutile-TiO_2 when it is calcined above ~550–600 °C. V_2O_5/TiO_2 samples using CVC-TiO_2 have better SCR activity than samples using commercial P25-TiO_2 (Fig. 1) because CVC-TiO_2 consists mainly of the anatase phase. Chin et al. [8] reported that TiO_2 that is prepared via CVC and composed of primarily anatase phase has good catalytic activity. When V_2O_5 is loaded onto CVC-TiO_2, the anatase peaks of the catalysts are of low intensity and broad. The peak intensities in the XRD patterns of the V_2O_5/CVC-TiO_2 samples suggest that they have not begun to crystallize under V_2O_5 loading concentrations of <7 wt.% and that the nanomaterials were predominantly in the amorphous phase.

Table 1
BET results for the pure CVC-TiO_2 and V_2O_5/CVC-TiO_2 samples.

	Pure CVC-TiO_2	1 wt.% V_2O_5/CVC-TiO_2	2 wt.% V_2O_5/CVC-TiO_2	5 wt.% V_2O_5/CVC-TiO_2	7 wt.% V_2O_5/CVC-TiO_2	10 wt.% V_2O_5/CVC-TiO_2
SSA (m^2/g)	153.91	259.72	256.30	250.97	268.56	250.61

The specific surface areas of the CVC-TiO_2 and V_2O_5-loaded CVC-TiO_2 samples were 153.91 and ~250–268 m^2/g, respectively (Table 1). This BET-analysis result is in good agreement with the results of our previously studies [22–24]. The SSAs of the V_2O_5/CVC-TiO_2 samples were significantly larger than that of pure CVC-TiO_2, which suggests that V_2O_5 is well-dispersed on the CVC-TiO_2 surface and is not crystallized. In particular, at 7 wt.%, the SSA was 268.56 m^2/g, which is very large; this sample is expected to have more active sites for surface reactions. The BET-analysis result is also in good agreement with the XRD peaks. In the HR-TEM images (Fig. 4), the V_2O_5/CVC-TiO_2 sample had only anatase and V_2O_5 lattices and was amorphous, while V_2O_5/P25-TiO_2 also had crystalline rutile TiO_2.

3.2.2. FT-IR results

All V_2O_5-loaded CVC-TiO_2 materials were analyzed for organic or inorganic byproduct bonds on their surfaces via their FT-IR spectra (Fig. 5). The hydroxyl group bands, which appear at ~3450–3440 cm^{-1}, and carboxyl acid bands, which include the formic acid bands and are at ~1680–1300 and ~2920–2830 cm^{-1} [21], were not affected by increased V_2O_5 content. The V_2O_5 band is evident at ~981 cm^{-1} in the FT-IR spectra.

The V_2O_5 band was not detected in the FT-IR spectra until 5 wt.% loading, which suggests that there are few bonds between V_2O_5 and the CVC-TiO_2 surface in this loading range. Above 7 wt.% V_2O_5, a distinct V_2O_5 band was detected in the FT-IR spectra; therefore, CVC-TiO_2 samples with greater than 7 wt.% V_2O_5 have more bonds between V_2O_5 and the CVC-TiO_2 surface owing to the conversion to polymeric or bulk crystallized V_2O_5. The FT-IR spectroscopy and XRD results suggest that the V_2O_5 in 7 wt.% V_2O_5/CVC-TiO_2 was not crystallized (i.e., not in the bulk phase) and was well-dispersed in the form of many polymeric and few monomeric phases; hence, the V_2O_5 peak was not evident in XRD but the bonding was detected in the FT-IR spectrum. However, at 10 wt.% V_2O_5, the intensity of the V_2O_5 band in the FT-IR spectrum increased, and a V_2O_5 peak appeared in the XRD pattern. This suggests that V_2O_5 crystallizes slightly and converts from the polymeric to a bulk phase when 10 wt.% or higher V_2O_5 is loaded on CVC-TiO_2. In addition, we suggest that the SCR catalytic activity results from these phenomena including the formation of more polymeric and even bulk (i.e., crystallized) V_2O_5 on the support material surface at high V_2O_5 loading. The 7 wt.% sample resulted in good catalytic activity due to the presence of more active sites in the V_2O_5, which comprised more polymers and fewer monomers. In a previous study [27], heterogeneous catalysts doped in the polymeric state onto support material (TiO_2) resulted in better catalytic activity by providing more active reaction sites on the catalyst surface than bulk doped catalysts.

3.2.3. Chemical components

The above results confirm that 7 wt.% V_2O_5/CVC-TiO_2 is optimal for SCR catalysis because it is mainly in the anatase phase and contains amorphous V_2O_5 that is well-dispersed on the sample surface and in the polymeric state. XPS analysis (Fig. 6) was performed on the 7 wt.% sample. The samples with V_2O_5 loaded onto CVC-TiO_2 show a better balance of V^{4+} and V^{5+} in the V_{2p} Gaussian-fitted curves than samples with P25-TiO_2 (Fig. 6). Furthermore, the presence of more V^{4+} in the CVC-TiO_2 samples than in the P25-TiO_2 samples suggests that more active sites (i.e., redox site V^{4+}—OH) are present for the catalyst surface reaction for SCR. The presence of mixed V^{4+} and V^{5+} supports the catalytic surface reaction because it enables high electrical conductivity, as reported previously [22]. The O_{1s} curves of 7 wt.% V_2O_5/TiO_2 revealed that the V_2O_5/CVC-TiO_2 sample contained more hydroxyl groups than the V_2O_5/P25-TiO_2 sample; this supports the presence of an increased number of acidic sites (i.e., V—OH) for SCR.

In the XPS surface atomic content results (Table 2), the content of atomic V increased with increasing V_2O_5 loading up to 10 wt.%. However, according to the XRD and FT-IR results, V_2O_5 began to transform to a bulk crystallized form from the polymeric and/or monomeric phases at 10 wt.% loading. The V_2O_5/CVC-TiO_2 samples had more surface atomic V content. The V/Ti ratios of the V_2O_5/CVC-TiO_2 samples were 0.01, 0.04, 0.11, 0.16, and 0.16, with increased V_2O_5 loading of 1, 2, 5, 7, and 10 wt.%, respectively. The ratio of the samples using P25-TiO_2 at 7 wt.% was 0.13. The V/Ti ratio was highest for 10 wt.% V_2O_5/CVC-TiO_2, but this catalyst performed NO_x conversion similarly to the 7 wt.% sample. Furthermore, the increased oxygen in the V_2O_5/CVC-TiO_2 catalysts enhances NO_x reduction.

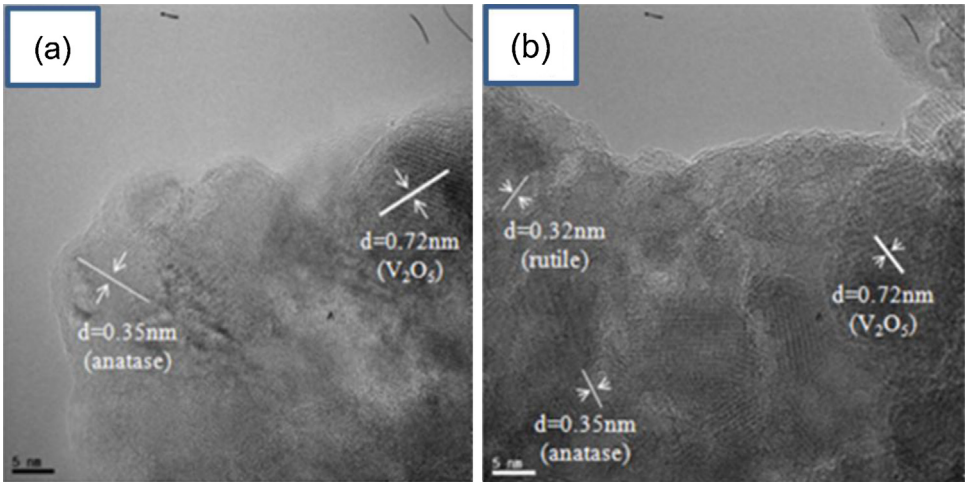

Fig. 4. HR-TEM images of 7 wt.% V_2O_5-loaded (a) CVC-TiO_2 and (b) P25-TiO_2.

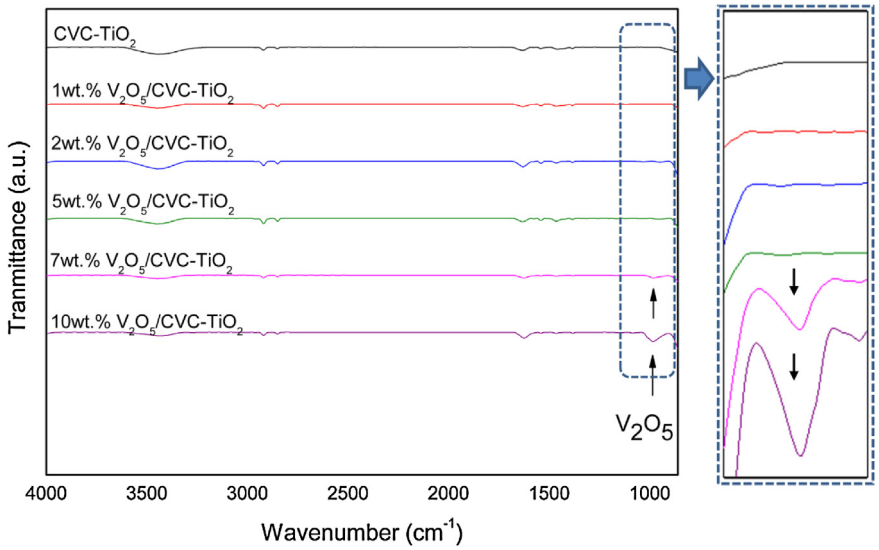

Fig. 5. FT-IR spectra of CVC-TiO_2 and V_2O_5/CVC-TiO_2 samples with different concentrations of V_2O_5 (i.e., 1, 2, 5, 7, and 10 wt.%).

Fig. 7 shows the vanadium elements dispersed onto CVC-TiO_2 and P25-TiO_2. We confirmed that the V_2O_5/CVC-TiO_2 contains more vanadium elements on the catalyst surface than V_2O_5/P25-TiO_2. The EDX mapping images were in good agreement with the V/Ti results obtained via XPS surface atomic content (Table 2), such as 0.16 and 0.13 for 7 wt.% V_2O_5/CVC-TiO_2 and 7 wt.% V_2O_5/P25-TiO_2, respectively. Furthermore, Fig. 7 shows that the vanadium elements were not aggregated, which correlates with the lack of V_2O_5 peak in the XRD pattern (Fig. 3). The EDX mapping images were also in good agreement with the XPS and XRD results.

3.2.4. Acidity and reduction capacity

The acidic sites on the surfaces of the samples were analyzed using NH_3-TPD. The NH_3-TPD result (Fig. 8) showed the trend and

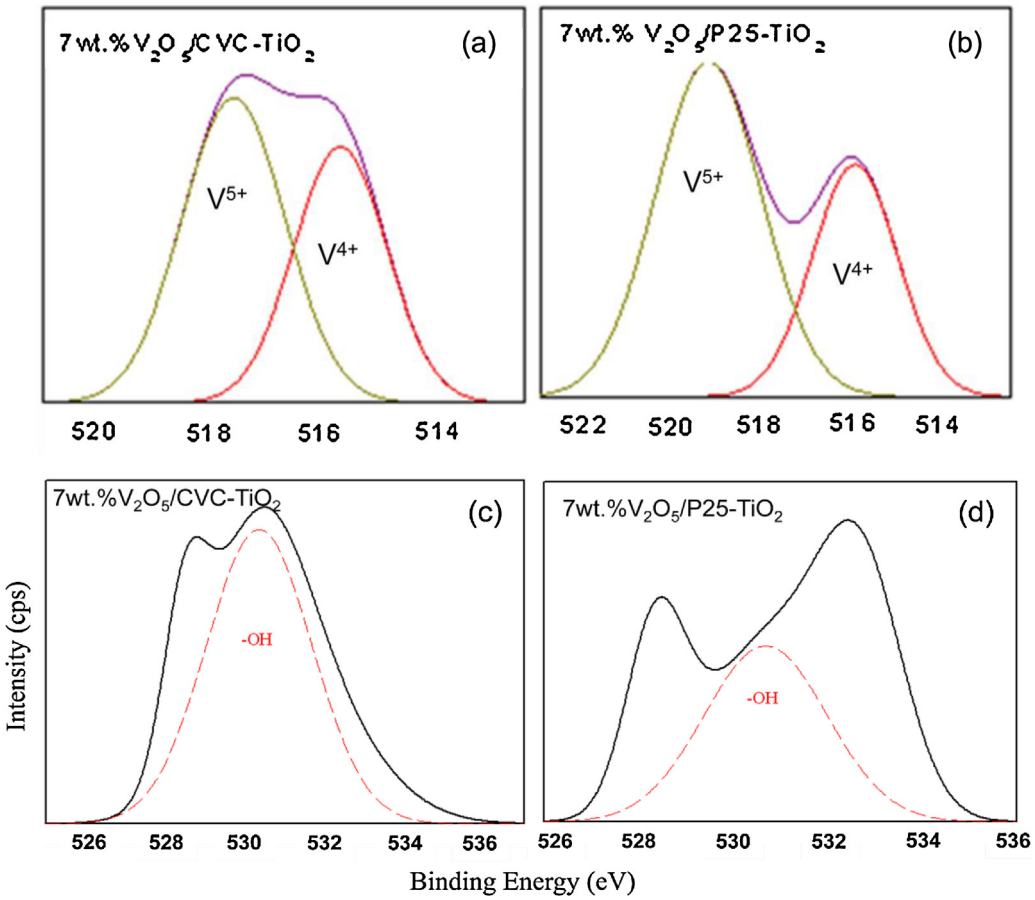

Fig. 6. XPS results for 7 wt.% V_2O_5/TiO_2: (a) V_{2p} of Gaussian-fitted curves of V_2O_5/CVC-TiO_2 and (b) V_2O_5/P25-TiO_2; (c) O_{1s} of Gaussian-fitted curves of V_2O_5/CVC-TiO_2 and (d) V_2O_5/P25-TiO_2.

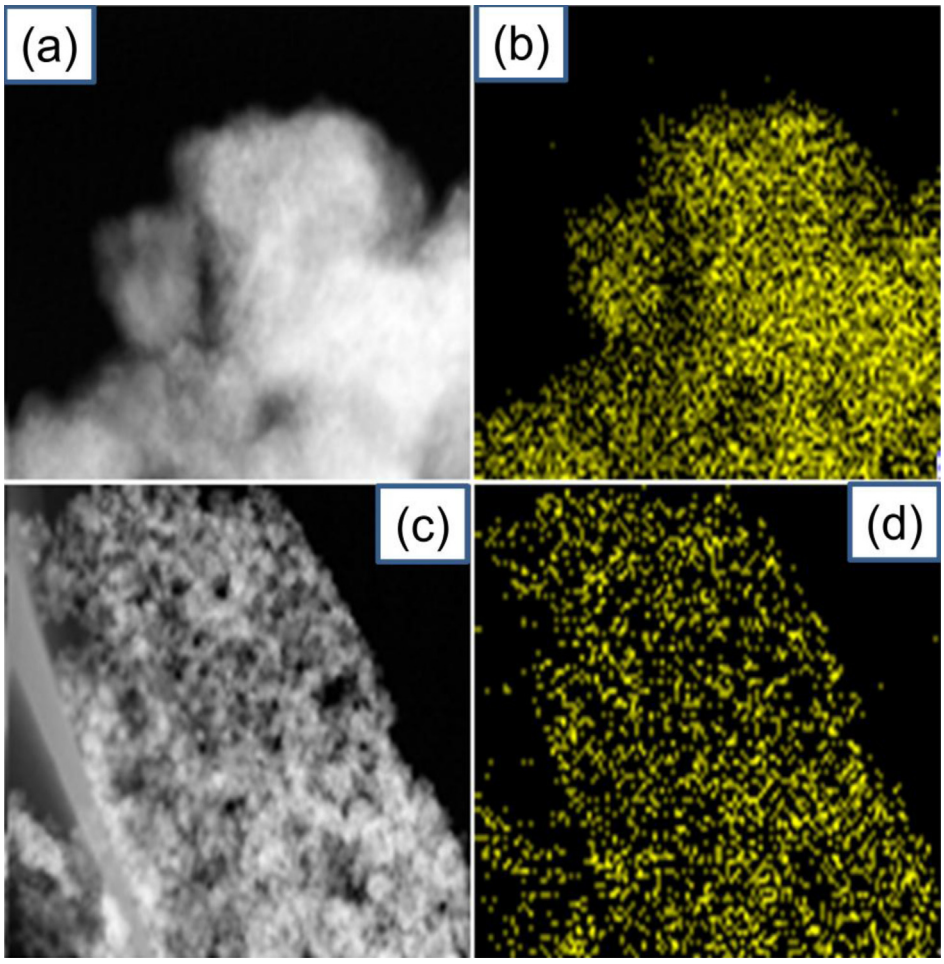

Fig. 7. EDX mapping of V_2O_5/TiO_2 catalysts: High-angle annular dark field image of (a) 7 wt.% V_2O_5/CVC-TiO_2 and (c) 7 wt.% V_2O_5/P25-TiO_2; V elemental spots of (b) 7 wt.% V_2O_5/CVC-TiO_2 and (d) 7 wt.% V_2O_5/P25-TiO_2.

quantity of acidic sites available for the catalyst surface reaction, and NH_3 desorption with increasing temperature from 0 to 600 °C. In the NH_3-TPD result, the TCD signal area of 7 wt.% V_2O_5/CVC-TiO_2 was larger than that of 7 wt.% V_2O_5/P25-TiO_2; this result suggests that the 7 wt.% V_2O_5/CVC-TiO_2 catalyst had more acidic sites to contribute to the catalytic activity than 7 wt.% V_2O_5/P25-TiO_2. In the NH_3-TPD result for 7 wt.% V_2O_5/CVC-TiO_2, the highest and second-highest peaks were at ~100 and ~290 °C, respectively. At 600 °C, the TCD peak dramatically increased, which suggests that many strongly acidic sites were present. In the NH_3-TPD result for 7 wt.% V_2O_5/P25-TiO_2, the highest peak was at ~100 °C, and the TCD signal intensity gradually decreased with increasing temperature from ~100 to 400 °C; the acidic sites were not evident above 440 °C.

Table 2
XPS surface atomic content (V, O, Ti) of pure CVC-TiO_2 and V_2O_5/CVC-TiO_2.

Samples	Surface atomic content (at.%)			
	V	Ti	O	V/Ti
Pure CVC-TiO_2	–	27.59	72.41	–
1 wt.% V_2O_5/CVC-TiO_2	0.61	27.08	72.37	0.01
2 wt.% V_2O_5/CVC-TiO_2	1.12	26.57	72.31	0.04
5 wt.% V_2O_5/CVC-TiO_2	2.76	25.04	72.20	0.11
7 wt.% V_2O_5/CVC-TiO_2	3.78	24.30	71.92	0.16
10 wt.% V_2O_5/CVC-TiO_2	5.01	23.46	71.53	0.21
Pure P25-TiO_2	–	28.96	71.04	–
7 wt.% V_2O_5/P25-TiO_2	3.50	25.03	71.47	0.13

Reducibility testing was performed via H_2-TPR (Fig. 9). In the H_2-TPR profile, we confirmed the initial reaction temperature, the highest reaction temperature of the TCD signal peak, and H_2 consumption with increasing temperature from 0 to 800 °C. The 7 wt.% V_2O_5/TiO_2 catalysts were used for H_2-TPR because they had the best SCR activity and feature appropriate characteristics for

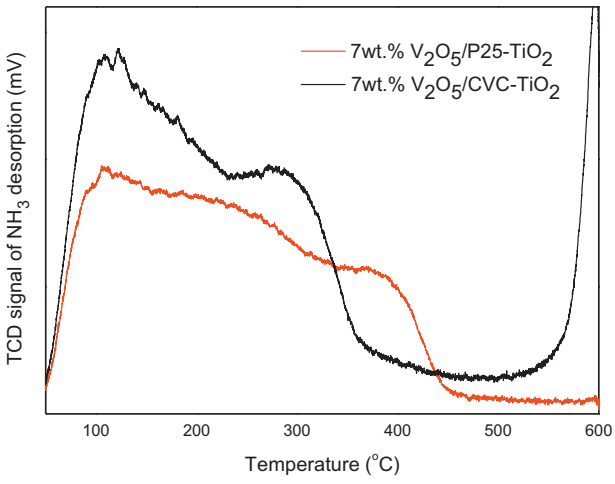

Fig. 8. NH_3-TPD result of 7 wt.% V_2O_5/TiO_2 catalysts.

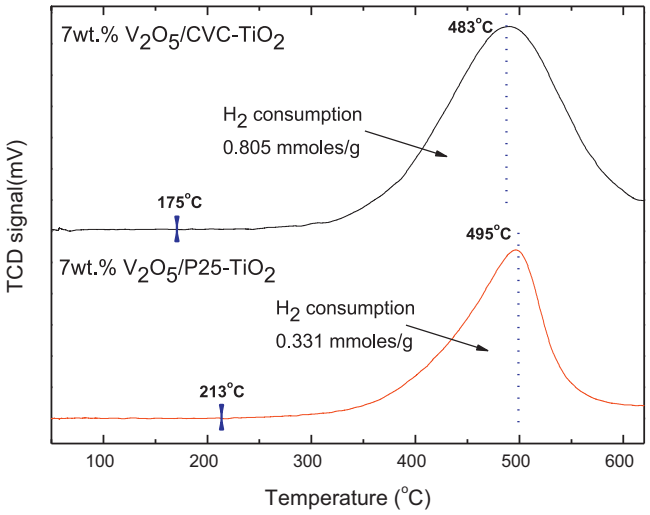

Fig. 9. H_2-TPR profiles of 7 wt.% V_2O_5/TiO_2 catalysts.

heterogeneous-catalyst surface reactions. In the H_2-TPR profile, the initial reaction temperatures and highest peaks for the V_2O_5/CVC-TiO_2 and V_2O_5/P25-TiO_2 catalysts were 175 and 483 °C and 213 and 495 °C, respectively. The H_2 consumption of the V_2O_5/CVC-TiO_2 catalyst at lower temperatures confirmed that this catalyst was more active toward SCR at lower temperatures than V_2O_5/P25-TiO_2. The TCD signal of the V_2O_5/CVC-TiO_2 catalyst was higher and broader resulting in a larger area. The quantities of H_2 consumed by the V_2O_5/CVC-TiO_2 and V_2O_5/P25-TiO_2 catalysts were 0.805 and 0.331 mmol/g, respectively; therefore, the H_2 consumption of the V_2O_5/CVC-TiO_2 catalyst was 2.42 times higher than that of V_2O_5/P25-TiO_2. This result implies that this catalyst consumed more H_2, which implies that a higher degree of reduction occurred on the surface of V_2O_5/CVC-TiO_2.

The primary reasons for the higher reducibility of the V_2O_5/CVC-TiO_2 catalyst include its higher surface area, increased oxygen concentration, well-dispersed vanadium, and balanced $V^{4+/5+}$ content that support many active sites, which contain acidic sites, during the reducing process. The high reducibility of the V_2O_5/CVC-TiO_2 catalyst contributes to its performance in the NH_3-SCR for NO_x removal. Sorrentino et al. [28] reported that catalysts with good reducibility in the H_2-TPR results had good catalytic activity toward the SCR process for DeNO$_x$, and the reducibility in TPR considerably correlates with the catalytic activity of the catalyst.

4. Conclusions

V_2O_5/TiO_2 catalysts were prepared by CVC and impregnation methods with varied concentrations of V_2O_5 (i.e., 1, 2, 5, 7, and 10 wt.%) and compared with the catalysts prepared using commercial P25-TiO_2. The catalytic activities of the catalysts were evaluated via NH_3-SCR of NO_x. In addition, the properties of the V_2O_5/TiO_2 catalysts were confirmed by XRD, BET, FT-IR spectroscopy, XPS, HR-TEM, EDX mapping, H_2-TPR, and NH_3-TPD analysis.

In the NH_3-SCR activity test, we confirmed the following four tendencies with respect to NO_x conversion with increased V_2O_5 loading: Firstly, all V_2O_5/TiO_2 catalysts prepared using CVC-TiO_2 had better NO_x conversion performance than catalysts prepared using P25-TiO_2; this is due to the beneficial surface properties of CVC-TiO_2 for heterogeneous catalysis, including larger specific surface area, mainly anatase-phase TiO_2, higher dispersion rate, and higher surface contents of V atoms, OH moieties, and lattice oxygen. Secondly, the V_2O_5 loading of CVC-TiO_2, which ranged from ~1 to 10 wt.%, was optimized at 7 wt.% for low-temperature (i.e., down to 200 °C) NO_x conversion. The NO_x conversion was about 96% at ~200–350 °C, which was attributed to the good dispersion of the predominantly polymeric and less monomeric vanadia phase, which has more active sites (that contain acidic sites), well-balanced $V^{4+/5+}$, which affects the electrical conductivity for catalysis, and outstanding reducibility. Thirdly, the SCR activity of the V_2O_5/CVC-TiO_2 catalysts increased with increasing V_2O_5 content from 1 to 7 wt.% at 200 °C because increased V_2O_5 loading leads to the formation of more and better-dispersed polymeric and monomeric V_2O_5. Fourth, the NO_x conversion of the 7 and 10 wt.% V_2O_5/CVC-TiO_2 catalysts were the same (i.e., 96% NO_x conversion) at 200 °C; this was likely due to the stabilization or reduction in the number of active sites for surface reactions of NO_x because polymeric and partly monomeric vanadia transforms to bulk (i.e., crystallized) vanadia as the V/Ti ratio increases.

We did not investigate the NH_3-SCR activity of NO_x in the presence of SO_2 and H_2O vapor in the present study. From stationary atmospheric pollution sources, NO_x removal in the presence of SO_2 and H_2O vapor is very important. The number of acidic sites is known to affect the stability of the catalyst surface in the presence of SO_2. In this study, we confirmed that V_2O_5/CVC-TiO_2 feature characteristics, including having more V and OH moieties and featuring vanadia primarily in the polymeric phase, that protect the catalyst against SO_2 poisoning. In future studies, the SCR catalyst prepared using CVC-TiO_2 and vanadia will be tested for catalytic activity and tolerance of SO_2 and H_2O vapor.

Acknowledgments

This work was supported by the Ministry of Environment (192-091-001) and the National Research Foundation of Korea Grant funded by the Korean Government (MSIP) (2013, University-Institute cooperation program).

References

[1] H. Phil, M. Reddy, P. Kumar, L. Ju, J. Hyo, Applied Catalysis B 78 (2008) 301–308.
[2] Y. Huang, Z.-Q. Tong, B. Wu, J.-F. Zhang, Journal of Fuel Chemistry and Technology 36 (2008) 616–620.
[3] H. Bosch, F.J.J.G. Janssen, Catalysis Today 2 (1988) 369–532.
[4] G. Busca, L. Lietti, G. Ramis, F. Berti, Applied Catalysis B 18 (1998) 1–36.
[5] I. Giakoumelou, C. Fountzoula, C. Kordulis, S. Boghosian, Journal of Catalysis 239 (2006) 1–12.
[6] M. Kang, J. Choi, Y.T. Kim, E.D. Park, C.B. Shin, D.J. Suh, J.E. Yie, Journal of Chemical Engineering 26 (2009) 884–889.
[7] V. Pârvulescu, P. Grange, B. Delmon, Catalysis Today 46 (1998) 233–316.
[8] S. Chin, E. Park, M. Kim, G.N. Bae, J. Jurng, Journal of Colloid and Interface Science 362 (2011) 470–476.
[9] S. Chin, J. Jurng, J.H. Lee, S.J. Moon, Chemosphere 75 (2009) 1206–1209.
[10] Z. Wang, C. Choi, J. Kim, B. Kim, Z. Zhang, Materials Letters 57 (2003) 3560–3564.
[11] H.A. Le, S.M. Chin, E.S. Park, L.T. Linh, G.N. Bae, J.S. Jurng, Chemical Vapor Deposition 17 (2011) 228–234.
[12] S. Chin, E. Park, M. Kim, J. Jeong, G.N. Bae, J. Jurng, Powder Technology 206 (2011) 306–311.
[13] G. Centi, E. Giamello, D. Pinelli, F. Trifiró, Journal of Catalysis 130 (1991) 220–237.
[14] J.W. Liu, Q. Sun, Y.C. Fu, J.Y. Shen, Journal of Colloid and Interface Science 335 (2009) 216–221.
[15] P. Courtine, E. Bordes, Applied Catalysis A 157 (1997) 45–65.
[16] I.E. Wachs, B.M. Weckhuysen, Applied Catalysis A 157 (1997) 67–90.
[17] G.C. Bond, Applied Catalysis A 157 (1997) 91–103.
[18] E. Park, H.A. Le, Y.S. Kim, S. Chin, G.N. Bae, J. Jurng, Materials Research Bulletin 47 (2012) 1040–1044.
[19] S.M. Chin, E.S. Park, M.S. Kim, J.S. Jurg, Powder Technology 201 (2010) 171–176.
[20] M.Y. Song, S. Chin, J. Jurng, Y.-K. Park, Ceramics International 38 (2012) 2613–2618.
[21] J. Araña, O. González Díaz, M. Miranda Saracho, J.M. Doña Rodríguez, J.A. Herrera Melián, J. Pérez Peña, Applied Catalysis B 36 (2002) 113–124.
[22] C. Tsang, A. Manthiram, Journal of the Electrochemical Society 144 (1997) 520–524.

[23] Y.S. Kim, M.Y. Song, E.S. Park, S. Chin, G.-N. Bae, J. Jurng, Applied Biochemistry and Biotechnology 168 (2012) 1143–1152.
[24] S. Chin, E. Park, M. Kim, G.-N. Bae, J. Jurng, Materials Letters 75 (2012) 57–60.
[25] A. Bellifa, D. Lahcene, Y.N. Tchenar, A. Choukchou-Braham, R. Bachir, S. Bedrane, C. Kappenstein, Applied Catalysis A 305 (2006) 1–6.
[26] G. Qi, R.T. Yang, Applied Catalysis B 44 (2003) 217–225.
[27] S.T. Choo, Y.G. Lee, I.S. Nam, S.W. Ham, J.B. Lee, Applied Catalysis A 200 (2000) 177–188.
[28] A. Sorrentino, S. Regaa, D. Sannino, A. Magliano, P. Ciambelli, E. Santacesaria, Applied Catalysis A 209 (2001) 45–57.
[29] A. Shi, X. Wang, T. Yu, M. Shen, Applied Catalysis B: Environmental 106 (2011) 359–369.